Design, Synthesis, and Characterization of a Fluoroprobe for Live Human Islet Cell Imaging of Serotonin 5-HT$_{1A}$ Receptor

Robert W. Garvey,[a] Enza Lacivita,*[b] Mauro Niso,[b] Beata Duszyńska,[c] Paul E. Harris,[a] and Marcello Leopoldo[b]

Mounting evidence suggests that the serotonin system serves in signal transmission to regulate insulin secretion in pancreatic islets of Langerhans. Among the 5-HT receptor subtype found in pancreatic islets, serotonin receptor 1 A (5-HT$_{1A}$) demonstrates a unique ability to inhibit β-cell insulin secretion. We report the design, synthesis, and characterization of two novel fluorescent probes for the 5-HT$_{1A}$ receptor. The compounds were prepared by conjugating the scaffold of the 5-HT$_{1A}$ receptor agonist 8-OH-DPAT with two fluorophores suitable for live-cell imaging. Compound **5a** {5-(dimethylamino)-N-[5-[(8- hydroxy-1,2,3,4-tetrahydronaphthalen-2-yl)(propyl)amino]pentyl]naphtalen-1-sulfonammide} showed high affinity for the 5-HT$_{1A}$ receptor ($K_i = 1.8$ nM). Fluoroprobe **5a** was able to label the 5-HT$_{1A}$ receptor in pancreatic islet cell cultures in a selective manner, as the fluorescence emission was significantly attenuated by co-administration of the 5-HT$_{1A}$ receptor antagonist WAY-100635. Thus, fluoroprobe **5a** showed useful properties to further characterize this unique receptor's role.

Introduction

Serotonin (5-hydroxytryptamine, 5-HT) plays the role of neurotransmitter in the central and the peripheral nervous systems and of a hormone in the gut.[1] 5-HT is present in islets of several mammalian species,[2,3] indicating a role for this biogenic amine in islet cell function. There are significant pre-prandial and post-prandial serum excursions of serotonin in healthy volunteers. Post-prandial 5-HT excursions are coincident with increases in serum insulin concentrations.[4] Nevertheless, the role of serotonin in regulating glucose-stimulated insulin secretion[5] has several remaining controversies. A confound to the better understanding of the role of 5-HT and its receptors (5-HTRs) in the regulation of glucose homeostasis is that fourteen different 5-HTR subtypes exist.[6] The distribution of 5-HTRs has been studied in rat and human islets.[7,8] The 5-HT$_{2A}$ and 5-HT$_{2B}$ receptors show high expression relative to the moderate expression of 5-HT$_{1A}$, 5-HT$_{1B}$, and 5-HT$_{3A}$ receptors.

The expression of 5-HT$_{1D}$, 5-HT$_{2C}$, 5-HT$_{3B}$, 5-HT$_4$, 5-HT$_{5A}$, 5-HT$_6$, and 5-HT$_7$ receptors was low to absent. An additional confound relates to how these receptors signal at the sub-cellular level and that intracellular 5-HT can also modulate β-cell insulin secretion.[9] Generally speaking, 5-HTRs are G-protein-coupled receptors, excepted 5-HT$_3$R. 5-HT$_4$, 5-HT$_6$, and 5-HT$_7$ receptors are coupled to Gs, which activates adenylyl cyclase (A.C.) to promote insulin secretion.[10] In opposition, 5-HT$_{1A/B/D}$ receptors are coupled to Gi, which inhibits A.C., thus probably inhibiting β-cell insulin secretion.[11] 5-HT$_{2A}$ and 5-HT$_{2C}$ receptors are coupled to Gq and are known to respectively promote[7] or inhibit[12] insulin secretion. It is important to note that to achieve its final effect on the regulation of glucose homeostasis, 5-HTRs (e.g., 5-HT$_{1F}$R) can also act on α-cells secreting glucagon, a hormone with action opposite to that of insulin.[13,14] Lastly, activation of the ligand-gated nonselective cation channel 5-HT$_3$R results in rapid depolarization, which suggests 5-HT$_3$R could potentially promote insulin granule exocytosis.[15] Current antipsychotic and antidepressant drugs have been demonstrated to affect the peripheral 5-HT system[6,16] and several studies have suggested the involvement of the serotonin system in glucose dysregulation.[17–19] These effects warrant further research on the effects of these drugs on the regulation of glucose homeostasis.

To better understand the expression and role of 5-HTRs in islets and their constituent cells, we have developed a novel fluorescent probe for 5-HT$_{1A}$R, suitable for live cell imaging. This report describes the design, synthesis, and validation of the probe and the study of cellular distribution of 5-HT$_{1A}$R among cultured human islets cells. Our results show that 5-HT$_{1A}$R and 5-HT$_{2A/B.R.s}$ can have non-overlapping vesicular distributions, a finding that may be relevant to their opposing actions on A.C. activity and possibly insulin secretion.[7]

[a] R. W. Garvey, Prof. P. E. Harris
Division of Endocrinology, Department of Medicine and Naomi Berrie Diabetes Center
Columbia University Medical Center, New York, NY■■postcode is missing!!■■(USA)

[b] Prof. E. Lacivita, Dr. M. Niso, Prof. M. Leopoldo
Dipartimento di Farmacia – Scienze del Farmaco
Università degli Studi di Bari Aldo Moro
via Orabona 4, 70125 Bari (Italy)
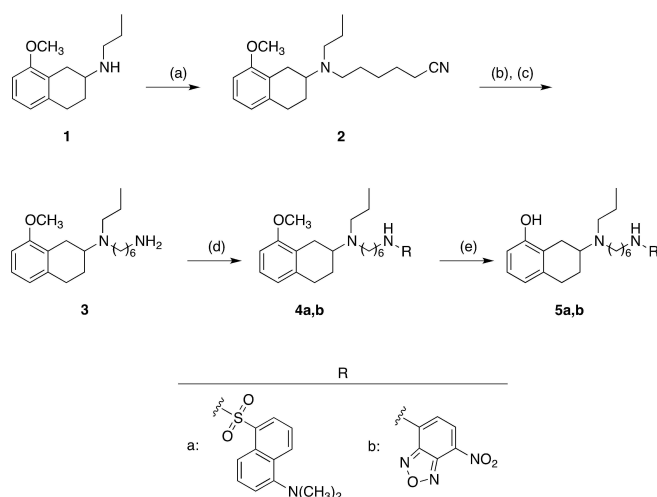E-mail: enza.lacivita@uniba.it

[c] Dr. B. Duszyńska
Department of Medicinal Chemistry
Maj Institute of Pharmacology
Polish Academy of Sciences
Smetna 12, 31-343 Krakow (Poland)

ChemMedChem

Research Article
doi.org/10.1002/cmdc.202100759

**Chemistry
Europe**
European Chemical
Societies Publishing

Results and Discussion

Design, synthesis, and fluorescent properties of compounds 5a,b

Over the years, several studies have reported the synthesis of small-molecule fluoroprobes for 5-HT$_{1A}$R. The design strategy encompassed the selection of a selective 5-HT$_{1A}$R ligand and subsequent functionalization with a linker in an area of the molecule known to tolerate substantial steric bulk and conjugation with a suitable fluorophore.[20] Following this strategy, we and others have identified various arylpiperazine-based 5-HT$_{1A}$R fluoroprobes, characterized by different 5-HT$_{1A}$R affinities, fluorescent properties, and fluorescence signal-to-noise ratios.[21–26] For our study, we designed a new series of fluoroprobes based on the standard 5-HT$_{1A}$R agonist 8-OH-DPAT.[27,28] Previous structure-activity relationship studies on 8-OH-DPAT showed that the replacement of one of the propyl groups with an alkyl group bearing in ω-position a bulky substituent did not affect high affinity for 5-HT$_{1A}$R.[29] Thus, we replaced one of the propyl groups of 8-OH-DPAT with a 6-aminohexyl substituent (compound **3**) to be conjugated with the fluorescent moieties dansyl (**5a**) and 7-nitrobenzofurazan (**5b**) that are characterized

by different excitation/emission wavelengths. The synthesis of the target fluoroprobes is depicted in Scheme 1. 8-Methoxy-2-propylamino-1,2,3,4-tetrahydronaphthalene (**1**)[30] was alkylated with 6-bromohexanenitrile to give the nitrile **2** which was reduced with borane methyl sulfide complex to yield the key amine **3**. Conjugation of the latter with 5-dimethylaminonaphthalene-1-sulfonyl chloride or 4-chloro-7-nitro-1,2,3-benzoxadiazole gave compounds **4a** and **4b**, respectively. Demethylation of these latter methoxy derivatives with boron tribromide afforded the target fluorescent compounds **5a** and **5b**, respectively.

The fluorescence spectra of compounds **5a,b** were determined in polar solvents (PBS buffer and ethanol) or chloroform as a model of lipophilic environment (Table 1). To determine the maximum absorption wavelength, for each compound was recorded the U.V./Vis absorption spectrum in the wavelength range between 190 nm and 700 nm. The emission spectra were recorded in the wavelength range between 300 and 800 nm, progressively exciting at values of λ included in the ±20 nm range with respect to the absorption λ$_{max}$. Both **5a** and **5b** were fluorescent, indicating that conjugation of the fluorophore to the pharmacophore moiety via a hexyl linker is not detrimental to the fluorescent properties.

Binding affinity at 5-HT$_{1A}$R of compounds 5a,b

The target fluorescent compounds were tested in radioligand binding assays to determine their affinity for 5-HT$_{1A}$R. The assay was performed via the displacement of the specific binding of [³H]-8-OH-DPAT at the cloned human 5-HT$_{1A}$R stably expressed in HEK293 cells. K_i data of the fluoroprobes **5a,b** and the reference 5-HT$_{1A}$R ligands 8-OH-DPAT and buspirone are listed in Table 1. Both compound **5a** and **5b** showed affinity at 5-HT$_{1A}$R in the nanomolar range, with compound **5a** showing slightly higher affinity than 8-OH-DPAT. In agreement with previous findings, the replacement of one propyl substituent on the basic nitrogen with a hexyl chain bearing in 6-position the fluorescent moiety was well tolerated. Based on the affinity values, we selected **5a** ($K_i = 1.8$ nM) for the subsequent labeling studies.

Scheme 1. Synthesis of the fluoroprobes **5a,b**: (a) 6-bromohexanenitrile, Na$_2$CO$_3$, acetonitrile, reflux, 80% yield; (b) borane-dimethyl sulfide complex, anhydrous THF, 5 h reflux; (c) MeOH, 3 N HCl, 1 h reflux, 76% yield; (d) a: 5-(dimethylamino)naphthalene-1-sulfonyl chloride, anhydrous CH$_2$Cl$_2$ r.t., 5 h, 30% yield. b: 4-chloro-7-nitrobenzofurazan, Na$_2$CO$_3$, abs. ethanol, 2 h, 48% yield; (e) 1 M BBr$_3$ in CH$_2$Cl$_2$, r.t. 3–4 h, 60–69% yield.

Table 1. 5-HT$_{1A}$R affinities and fluorescence properties of the target and reference compounds.

Compd	5-HT$_{1A}$R affinity K_i [nM] ± SD[a]	Fluorescent properties PBS buffer		EtOH		CHCl$_3$	
		λ$_{ex}$ [nm]	λ$_{em}$ [nm]	λ$_{ex}$ [nm]	λ$_{em}$ [nm]	λ$_{ex}$ [nm]	λ$_{em}$ [nm]
8-OH-DPAT	3.2[b]	–	–	–	–	–	–
buspirone	27.9 ± 1.7	–	–	–	–	–	–
5a	1.8 ± 0.2	334	540	335	516	340	482
5b	10 ± 1	490	560	470	535	451	524

[a] Each compound was tested in triplicate; data are the mean of two separate experiments. [b] Taken from Millan et al.[31]

ChemMedChem

Research Article
doi.org/10.1002/cmdc.202100759

Chemistry
Europe
European Chemical
Societies Publishing

Fluoroprobe 5a colocalizes with and binds preferentially to 5-HT$_{1A}$R-positive cells

Compound **5a** (GMA 9) was used to evaluate the expression and distribution of 5-HT$_{1A}$R in monolayer cultures of dissociated human islet cells developed using the two-dimensional human β-cell culture system previously reported.[32] To visualize the cellular and subcellular distribution of **5a** fluorescent staining in live human islet cells, we incubated day 5 cultures with different concentrations of the fluoroprobe ranging from 20 nM to 10 μM (data not shown). The best results were obtained using 10 μM **5a** and, thus, the cultures for fluorescent microscopy were prepared and digitally captured the blue-fluorescent emission signals (Figure 1).

We found that **5a** fluoresced at the expected emission wavelengths and gave a vesicular pattern within the islet cells' cytoplasm. The population of islets cells showed three main subpopulations with respect to vesicle frequency: 1) high, with greater than 150 vesicles/cell ratio, 2) intermediate, with about 150 to 50 vesicles/cell ratio, and 3) fewer than 50 vesicles/cell ratio. The modal vesicular diameter was around 0.8 μm ($n = 200$). Within the cytoplasm, vesicles were distributed in the perinuclear space as well in the ██periplasmic█*OK?*█ space.

Next, to validate **5a** specificity for 5-HT$_{1A}$R, **5a** fluorescence was assessed in competition with various concentrations of non-fluorescent WAY-100635 maleate, an established 5-HT$_{1A}$R antagonist.[33,34] Live islet cell cultures were treated with **5a** and WAY-100635, in a DMSO vehicle, in increasing concentrations (2% DMSO vehicle only, 50 μM WAY-100635, 400 μM WAY-100635) (Figure 2).

As expected, **5a** fluorescent emission was attenuated by the addition of the 5-HT$_{1A}$R antagonist, affirming **5a** displacement by WAY-100635. The vesicular **5a** signal intensity decreased as
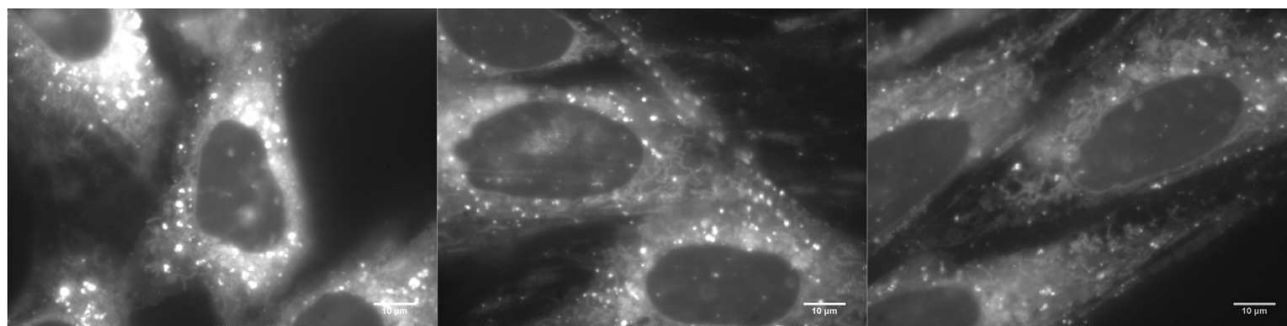

Figure 1. Islet cell distribution of 5-HT$_{1A}$R using **5a**. Live islet cells were incubated with the 5-HT$_{1A}$R fluoroprobe **5a** (10 μM final concentration) for 40 minutes at room temperature, washed, and overlayed with imaging media. Cells were imaged by their fluorescent blue emission (excitation 365–405 nm, emissions > 420 nm), represented here as a greyscale image. Islet cells were imaged on day 5 of culture. The scale bar represents 10 μm.
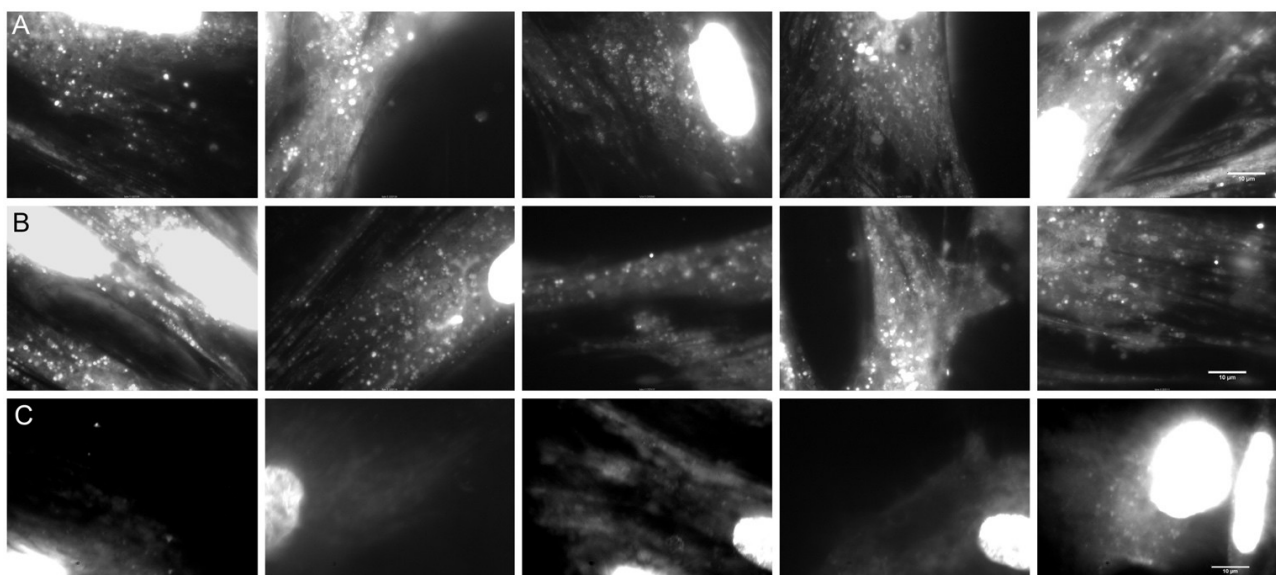

Figure 2. Specificity of binding of **5a** to 5-HT$_{1A}$R in Islet cells. Live islet cells were incubated with the 5-HT$_{1A}$R fluoroprobe **5a** (10 μM final concentration) and 2% DMSO vehicle only (Panels A, top), or plus 50 μM WAY-100635, (Panels B, middle), or plus 400 μM WAY-100635 (Panels C, bottom), washed and digitally imaged by their fluorescent blue emission (excitation 365–405 nm, emissions > 420 nm. The fluorescent blue nuclear stain DAPI was also added to aid in identifying cells with diminished vesicular staining. The scale bar represents 10 μm.

ChemMedChem

Research Article
doi.org/10.1002/cmdc.202100759

Chemistry
Europe
European Chemical
Societies Publishing

WAY-100635 concentration increased. To better quantify the specificity of **5a** vesicular binding, machine counting of the fluorescence vesicular signal in islet cell cytoplasm was compared in competition with WAY-100635 in live islet cell cultures. Machine counting confirmed displacement of **5a** by WAY-100635 as seen by the decrease in the vesicular fluorescent intensity and, as a result, the number of countable vesicles per 100 μm² of cytoplasm in small, large, and total vesicles (Figure 3). We can speculate that **5a** crossed plasma membrane by passive diffusion, as the mechanism of cellular uptake has not been elucidated yet.

5-HT$_{1A}$R and insulin colocalize in the vesicles of cultured β-cells

Insulin-containing β-cell vesicles have been reported to maintain a resting pH between 5.9–6.2.[35] To gather further information about the distribution of 5-HT$_{1A}$R in human islets cells, we took advantage of the pH of insulin-containing β-cell vesicles by staining cells with LysoTracker Red DND-99, a fluorescent probe specific for acidic organelles. Live cell cultures were treated with LysoTracker Red DND-99, **5a**, and H.C.S. NuclearMask Deep Red nuclear stain. Merged pseudocolor images of LysoTracker, **5a**, and H.C.S. nuclear stained cell cultures revealed the localization of acidic vesicles, nuclei, and 5-HT$_{1A}$R (Figure 4). Registered and merged pseudocolor images
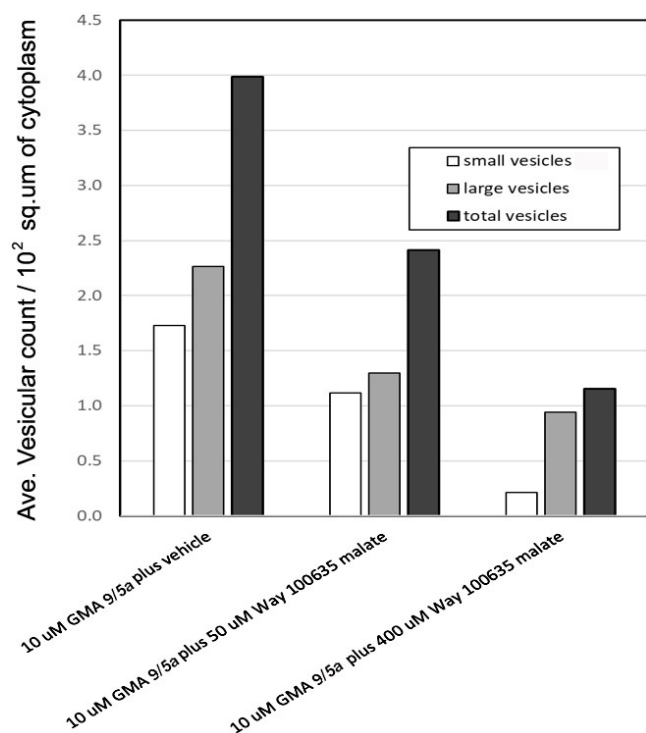
of islets cells reveal colocalization of 5-HT$_{1A}$R and acidic vesicles in many large cell vesicles, although many small vesicles show affinity for just one fluorescent marker. To obtain further evidence that 5-HT$_{1A}$R was associated with insulin-containing vesicles, we studied the distribution of vesicles containing Zn^{+2} ions as a surrogate marker for insulin hexamer.[32,36,37] Islet cell cultures were stained with FluoZin-3 AM and **5a** to reveal possible colocalization of Zn^{+2} and 5-HT$_{1A}$R (Figure 5■■*Changed from* Figure 6 *here; OK?*■■ and Supporting Information Figure S1). The resulting pseudocolor images of FluoZin-3 AM, **5a**, and H.C.S. nuclear stain cell cultures affirm colocalization of insulin bound zinc and the 5-HT$_{1A}$R **5a** fluoroprobe in some, but not all cell vesicles. Because 5-HT$_{1A}$R **5a** fluoroprobe and Hoechst 33342 share similar excitation and emission profiles but different subcellular distributions (i.e., vesicular versus nuclear), we developed a simpler protocol where live cells were stained with 5-HT$_{1A}$R **5a** fluoroprobe, Hoechst 33342 nuclear stain and FluoZin-3 AM and imaged in the visible blue and green wavelengths (Supporting Information Figure S1). We observed islets cells that stained for both 5-HT$_{1A}$R and Zn^{+2}, cells that stained for 5-HT$_{1A}$R alone and cells that stained for Zn^{+2} alone.

5-HT$_{1A}$R and dopamine colocalize in vesicles of cultured β-cells

We have shown that β-cells serve as the principal storage site for dopamine in the pancreas[32] and release both insulin and dopamine in response to glucose challenge.[38] Since agonism at both dopamine D$_2$ receptor and 5-HT$_{1A}$R might inhibit insulin secretion, we examined whether dopamine and 5-HT$_{1A}$ receptors could be found in the same β-cell vesicles. Monolayers of dissociated live human islet cell cultures were treated with **5a**, H.C.S. nuclear stain, and NeuroSensor 521, a fluorescent probe for dopamine, and examined by fluorescent microscopy (Figure 6). The resulting pseudo color images demonstrated colocalization of 5-HT$_{1A}$R and dopamine in some but not all imaged cells.

Vesicular 5-HT$_{1A}$R and 5-HT$_{2A}$R localize differently in cultured islet cells

Monolayers of dissociated human islet cell cultures were treated with **5a**, Hoechst 33342 nuclear stain and CellAura 5-HT$_{2A/2B}$ – a commercial fluoroprobe antagonist of 5-HT$_{2A/2B}$ receptors (Figure 7).

Pseudocolor images revealed that the vesicular localization of 5-HT$_{1A}$R and 5-HT$_{2A/2B}$ receptors were often, but not exclusively, distinct. Further, it appeared that 5-HT$_{1A}$R might localize near the plasma membrane while 5-HT$_{2A}$ receptors maintain a perinuclear localization.

To corroborate our observations regarding the specificity of staining of the 5-HT$_{1A}$R **5a** fluoroprobe, we performed immunochemistry on fixed islet cell cultures and formaldehyde-fixed paraffin-embedded whole pancreas tissue. Samples were

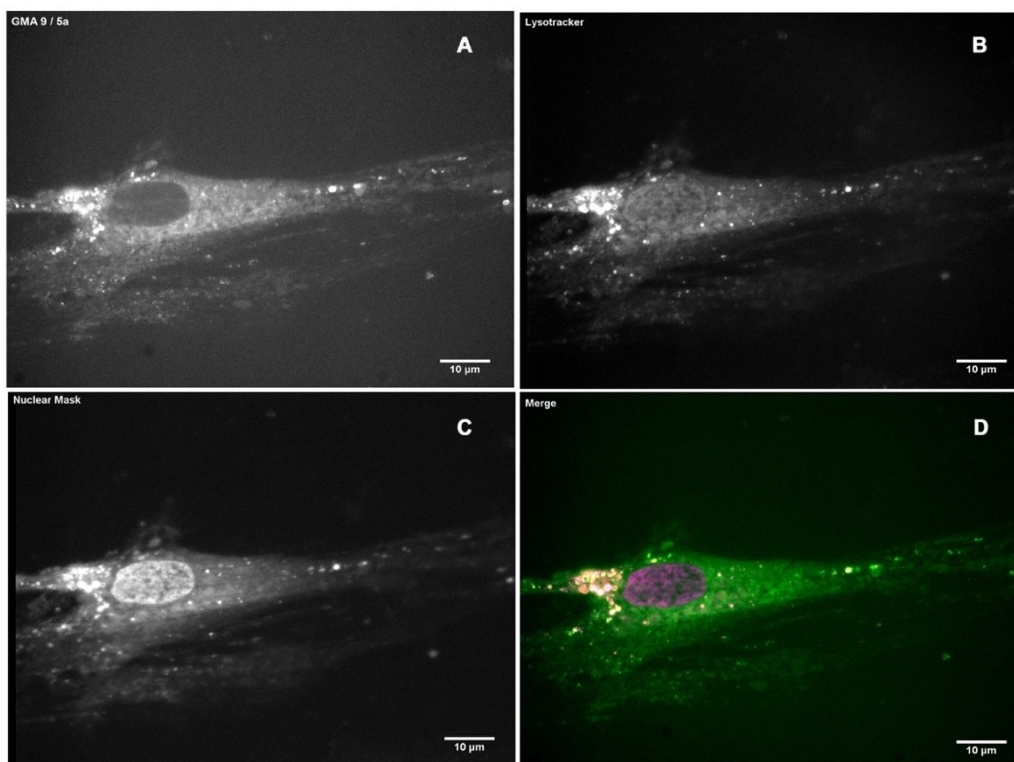**Figure 3.** Displacement of 5-HT$_{1A}$R fluoroprobe **5a** by WAY-100635. Live islet cell cultures were incubated in **5a** and increasing concentrations of WAY-100635 and imaged by their blue-fluorescent signal. Machine counting of vesicles revealed a reduction in the countable number of both small (<0.5 μm²), large (>0.5 μm².) and total vesicles

ChemMedChem

Research Article
doi.org/10.1002/cmdc.202100759

Chemistry Europe
European Chemical
Societies Publishing

Figure 4. Islet cell colocalization of 5-HT$_{1A}$R using **5a** and acidic vesicles. Live islet cells were incubated with the 5-HT$_{1A}$R fluoroprobe **5a** (10 μM final concentration) for 40 minutes at room temperature, washed, and overlayed with imaging media. Cells were imaged first by their fluorescent blue emission (A) (excitation 365–405 nm, emissions > 420 nm) using a U.V. source, next, using a broadband white light source, LysoTracker Red DND-99 (excitation 577 nm, emission 590 nm) (B) and (C) H.C.S. Nuclear Mask Deep Red (excitation 638 nm, emission 686 nm). A composite pseudocolor image (D) shows 5-HT$_{1A}$R staining in green, Acidic vesicles in red, and nuclear staining in purple. Colocalization of 5-HT$_{1A}$R and acidic vesicles is shown as a yellow signal. Islet cells were imaged on day 5 of culture.

immunostained for 5-HT$_{1A}$R, insulin, and DAPI nuclear stain (Figure 8). Because agonism at 5-HT receptors can also modulate glucagon secretion, a hormone which opposes insulin by stimulating hepatic glucose production, in pancreatic α-cells,[14] we also examined 5-HT$_{1A}$R and glucagon staining patterns (Figure 8).

Merged-color images confirm that glucagon or insulin and 5-HT$_{1A}$R immunoreactivity colocalized in some cell vesicles, consistent with previous studies[39] and the live cell staining experiments with the **5a** fluoroprobe. Immunostaining was repeated on formaldehyde-fixed paraffin-embedded rat pancreas tissue. Rat pancreas tissue images (see Supporting Information Figure S2, S3, and S4) revealed a similar pattern of 5-HT$_{1A}$R or 5-HT$_{2A}$R and insulin colocalization to human samples.

Conclusion

Starting from the scaffold of the HT$_{1A}$R agonist 8-OH-DPAT, we designed two new fluoroprobes by replacing one of the propyl groups with a hexamethylene chain bearing in ω-position the dansyl and 7-nitrobenzofurazan fluorophores, as their excitation wavelengths are compatible with imaging in living cells. The two fluorescent compounds **5a,b** have nanomolar affinity at 5-HT$_{1A}$R, with compound **5a** showing slightly higher affinity than

8-OH-DPAT ($K_i = 1.8$ nM vs. 3.2 nM). We selected compound **5a** to image 5-HT$_{1A}$Rs expressed in cultures of living human islet β-cells. Interestingly, compound **5a** selectively labeled the 5-HT$_{1A}$R, as the fluorescence emission was significantly attenuated by co-administration of the 5-HT$_{1A}$R antagonist WAY-100635. Using compound **5a**, we demonstrated that 5-HT$_{1A}$R expression is shared by β and α cells of human islets and is particularly evident in islet cell vesicles, a distribution similar to that of other neurotransmitter receptors in islet β-cells.[36] Compound **5a** emerged as a fluoroprobe to visualize 5-HT$_{1A}$R in living cells. The ability to image 5-HT$_{1A}$R in live cells and manipulate them pharmacologically in real-time provides the opportunity to visualize receptor expression and trafficking. Such studies may lead to a better understanding of the roles of these receptors in glucose homeostasis.

Experimental Section

Chemistry

Chemicals were purchased from Sigma-Aldrich and T.C.I. Chemicals. Unless otherwise stated, all chemicals were used without further purification. Column chromatography was performed with 1:30 Merck silica gel 60 A (63–200 μm) as the stationary phase. ^{1}H N.M.R. spectra were recorded at 300 MHz on a Varian Mercury-VX
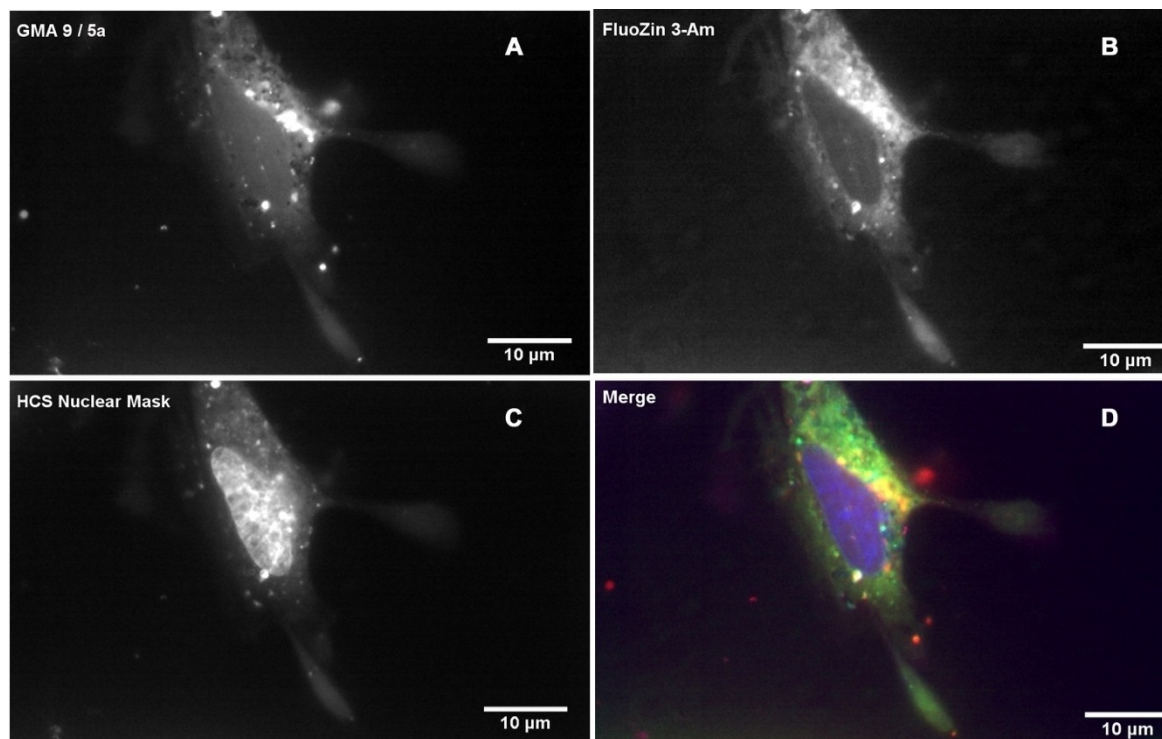
ChemMedChem

ResearchArticle
doi.org/10.1002/cmdc.202100759

Chemistry
Europe
European Chemical
Societies Publishing

Figure 5. Islet cell colocalization of 5-HT$_{1A}$R using **5a** and insulin hexamer-bound Zn^{+2}. Live islet cells were incubated with the 5-HT$_{1A}$R fluoroprobe **5a** (10 μM final concentration), FluoZin-3 AM and H.C.S. nuclear Mask Deep Red for 40 minutes at room temperature, washed, and overlayed with imaging media. Cells were imaged first by their fluorescent blue emission (A) (excitation 386.nm, emissions > 420 nm) using a U.V. source (350–400 nm), next, using a broadband white light source, FluoZin-3 AM (B) (excitation 494 nm, emission 516 nm) (C) and H.C.S. Nuclear Mask Deep Red (Bottom greyscale panel) (excitation 638 nm, emission 686 nm) were visualized. A composite pseudocolor image (D) shows 5-HT$_{1A}$R staining in green, FluoZin-3 AM Zn^{+2} in red, and nuclear staining in purple. Colocalization of 5-HT$_{1A}$R and insulin-hexamer bound Zn^{+2} is shown as a yellow signal. Islet cells were imaged on day 5 of culture. The scale bar represents 10 μm.
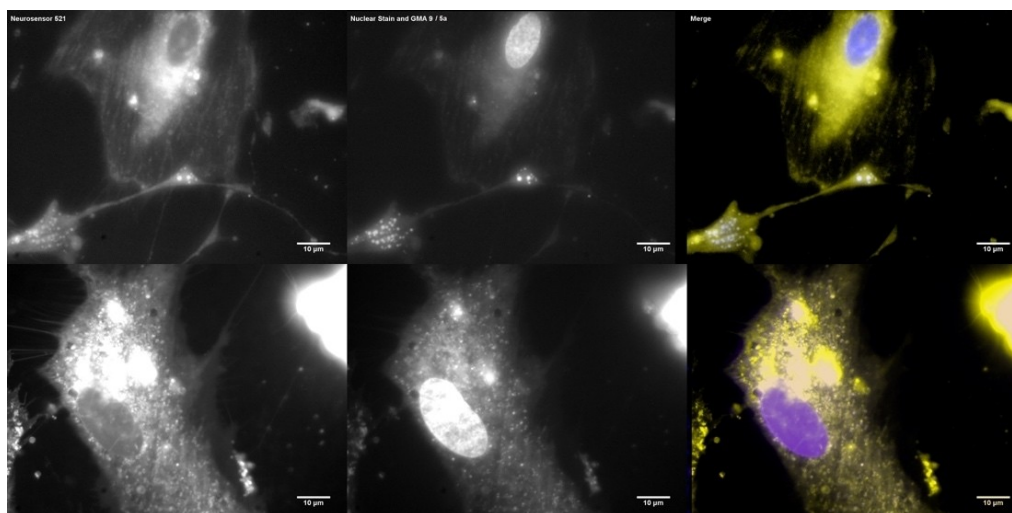

Figure 6. Representative islets cells showing different patterns of 5-HT$_{1A}$R fluoroprobe **5a** and NeuroSensor 521 dopamine probe staining. Live islet cells were incubated with NeuroSensor 521 (excitation 488 nm, emission 521 nm) (Left panels) and the 5-HT$_{1A}$R fluoroprobe **5a** and Hoechst 33342 nuclear stain (Middle panels). Composite pseudocolor images (Right panels) show overlapping blue (**5a** and nuclear stain) and yellow (NeuroSensor 521) signals in white.

spectrometer. All spectra were recorded on free bases. All chemical shift values are reported in ppm (δ). Recording of mass spectra was done on an HP6890-5973 MSD gas chromatograph/mass spectrometer; only significant m/z peaks, with their percentage of relative intensity in parentheses, are reported. ESI-MS/MS analyses were performed with an Agilent 1100 Series LC-MSD trap System V.L. workstation. All spectra were in accordance with the assigned structures. The purity of compounds **5a,b** has been assessed by RP-
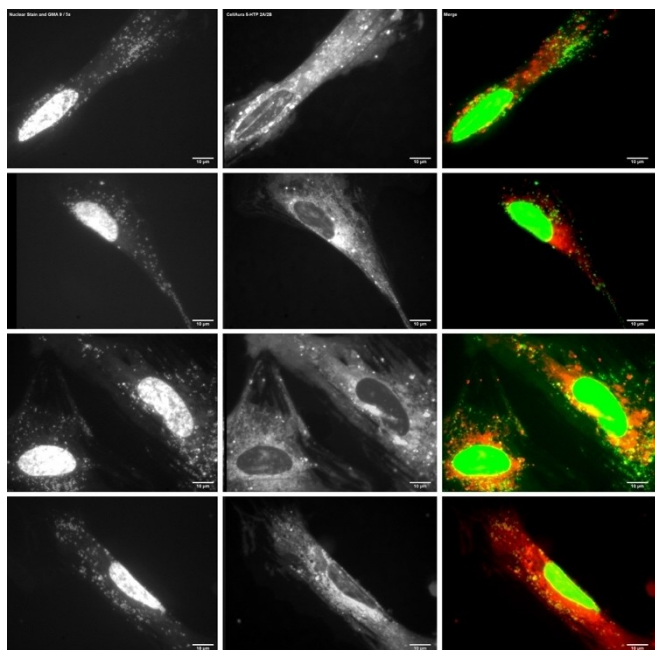
Figure 7. Representative islets cells show different patterns of 5-HT$_{1A}$R (**5a**) and 5-HT$_{2A/2B}$ receptor (CellAura) vesicular staining. Live islet cell cultures were incubated with the 5-HT$_{1A}$R fluoroprobe **5a** and Hoechst 33342 nuclear stain (Left panels) and CellAura 5-HT$_{2A/2B}$ (excitation 633 nm and 650 nm emission). Merged composite pseudocolor images (Right panels) show overlapping green (**5a** and nuclear stain) and red (5-HT$_{2A/2B}$ receptors) signals in yellow. The scale bar represents 10 μm.
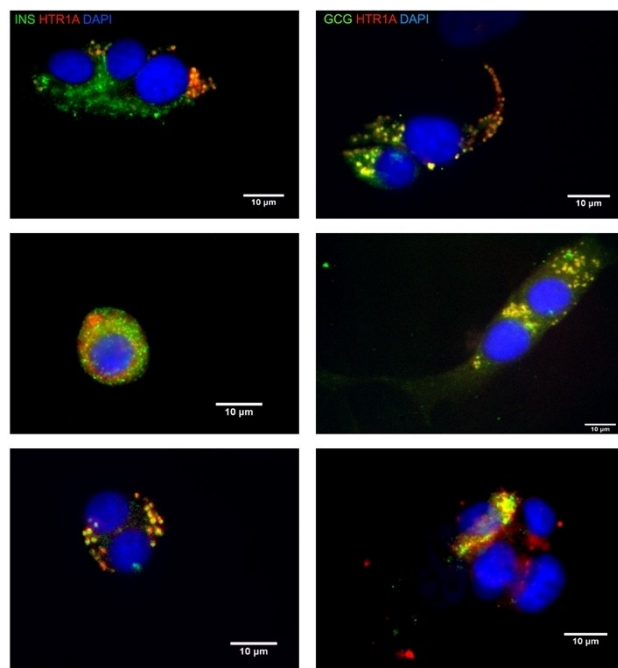

Figure 8. Overlapping and non-overlapping distributions of vesicular insulin or glucagon with 5-HT$_{1A}$R in human islet cell cultures. Cultures of human islet cells were fixed for immunohistochemistry with anti-insulin, anti-glucagon and anti 5-HT$_{1A}$R antibodies. Nuclei were counterstained with DAPI and imaged. The left panels are the merged pseudocolour images from a single focal plane obtained from photographs prepared in each channel (DAPI-blue, anti-insulin-green, anti 5-HT$_{1A}$R -red). The right panels are pseudocolour images of cells analyzed for glucagon staining (DAPI-blue, anti-glucagon-green, anti 5-HT$_{1A}$R -red). Overlapping signals are shown in yellow. The scale bar represents 10 μM.

HPLC analysis on an Agilent 1260 Infinity Binary L.C. System equipped with a diode array detector using a Phenomenex Gemini RP-18 column, (250×4.6 mm, 5 μm particle size). The compounds were isocratically eluted with CH$_3$CN/H$_2$O/Et$_3$N, 80:20:0.01, v/v at a flow rate of 1 mL/min and showed ≥95% purity. The purity of compounds was further assessed by gradient elution. The mobile phase consisted of 0.025% formic acid and 1 mM NH4OAc in water/ACN (95:5, v/v, solvent A) and 0.025% formic acid and 1 mM NH4OAc in ACN/water (95:5, v/v, solvent B). Linear gradient elution started from 90% A to 90% B within 5 min followed by isocratic elution (3 min) at 90% B. The flow rate was 1 mL/min.

8-Methoxy-2-[(6-cyanohexyl)propylamino]-1,2,3,4-tetrahydro-naphthalene (2). A stirred mixture of 6-bromohexanenitrile (0.67 g, 3.8 mmol), 8-methoxy-2-propylamino-1,2,3,4-tetrahydronaphtha-lene (**1**) (0.70 g, 3.2 mmol) and K$_2$CO$_3$ (0.55 g, 4.0 mmol) in acetonitrile was refluxed overnight. After cooling, the mixture was evaporated to dryness and H$_2$O (30 mL) was added to the residue. The aqueous phase was extracted with AcOEt (2×30 mL). The collected organic layers were dried over Na$_2$SO$_4$ and evaporated under reduced pressure. The crude residue was chromatographed (CHCl$_3$/MeOH, 19:1, as eluent) to afford pure compound **2** as a pale-yellow oil (0.80 g, 80% yield). ^{1}H NMR (CDCl$_3$): δ 0.89 (t, 3H, $J=$ 7.2 Hz), 1.43–1.56 (m, 3H), 1.57–1.76 (m, 4H), 1.88–1.98 (m, 2H), 2.32–2.41 (m, 4H), 2.46–2.54 (m, 4H), 2.81–2.94 (m, 4H), 3.82 (s, 3H), 6.65 (dd, 2H, $J=$7.7 and 8.0 Hz), 7.08 (t, 1H, $J=$8.0 Hz). GC-MS m/z 315 (M$^+$+1, 5), 314 (M$^+$, 23), 285 (59), 232 (56), 161 (100).

2-[(6-Aminohexyl)propylamino]- 8-methoxy-1,2,3,4-tetrahydro-naphthalene (3). Borane-methyl sulfide complex as 10.0 M BH$_3$ in excess methyl sulfide (0.8 mL, 8 mmol) was dropped into an ice-cooled solution of nitrile **2** (0.80 g, 2.55 mmol) in anhydrous T.H.F. (20 mL), under stirring. After being refluxed for 4 h, the reaction

mixture was cooled at −10 °C and MeOH was added dropwise very carefully until gas evolution ceased. The mixture was treated with 3 N HCl (20 mL) and was refluxed for 1 h. After cooling, the mixture was alkalized with 3 N NaOH and extracted with AcOEt (2×50 mL). The collected organic layers were dried over Na$_2$SO$_4$ and the solvent was evaporated under reduced pressure to give the pure amine as a colorless oil (0.62 g, 76% yield). ^{1}H NMR (CDCl$_3$): δ 0.88 (t, 3H, $J=$ 7.2 Hz), 1.32–1.40 and 1.42–1.52 (m, 10H), 1.73 (br s, 2H, D$_2$O exchanged), 1.97–2.02 (m, 1H), 2.41–2.56 and 2.65–2.71 (m, 8H), 2.83–2.96 (m, 4H), 3.81 (s, 3H), 6.67 (dd, 2H, $J=$7.7 Hz), 7.09 (t, 1H, $J=$7.7 Hz). GC-MS m/z 319 (M$^+$+1, 4), 318 (M$^+$, 15), 289 (38), 232 (87), 161 (100).

5-(Dimethylamino)-N-[5-[(8-methoxy-1,2,3,4-tetrahydronaphntha-len-2-yl)(propyl)amino]pentyl]naphtalen-1-sulfonammide (4a). To 5-dimethylaminonaphthalene-1-sulfonyl chloride (0.11 g, 0.4 mmol) dissolved in anhydrous CH$_2$Cl$_2$ (20 mL) a solution of amine **3** (0.25 g, 0.8 mmol) in the same solvent (10 mL). The reaction mixture was stirred at room temperature for 5 h. Subsequently, the mixture was first washed with H$_2$O (2×20 mL) and then with brine (20 mL). The separated organic layer was dried over anhydrous Na$_2$SO$_4$ and concentrated in vacuo. The crude residue was chromatographed with CHCl$_3$/AcOEt (1:1) as eluent, to give **4a** as a pale-yellow semisolid (0.07 g, 30% yield). 1H NMR (CDCl$_3$): δ 0.88 (t, 3H, $J=$ 7.3 Hz), 1.33–1.42 and 1.53–1.78 (m, 12H), 1.92–1.97 (m, 1H), 2.34–2.42 (m, 6H), 2.77–2.99 (m+s, 10H), 3.81 (s, 3H), 4.54 (br s, 1H, D$_2$O exchanged), 6.67 (dd, 2H, $J=$7.8 Hz), 7.07 (t, 1H, $J=$7.8 Hz), 7.17 (d, 1H, $J=$7.3 Hz), 7.50–7.56 (m, 2H), 8.23–8.29 (m, 2H), 8.52 (d, 1H, $J=$

8.8 Hz). HRMS (ESI$^+$) calcd for [(C$_{32}$H$_{45}$N$_3$O$_3$S+H]$^+$: 552.3254, found: 552.3247.

N-[5-[(8-Methoxy-1,2,3,4-tetrahydronaphthalen-2-yl)(propyl)amino]pentyl]-7-nitrobenzene[c][1,2,5]oxadiazol-4-sulfonamide (4b). To 4-chloro-7-nitro-1,2,3-benzoxadiazole (0.03 g, 0.17 mmol) dissolved in absolute ethanol (4 mL), a solution of amine **3** (0.09 g, 0.17 mmol) in a 1:1 mixture of CH$_3$CN and EtOH (4 mL). The reaction mixture was stirred at room temperature for 2 h. Then, the solvent was removed under reduced pressure and the residue taken up with a saturated aqueous solution of Na$_2$CO$_3$ (15 mL) and extracted with CH$_2$Cl$_2$ (3×15 mL). The separated organic layers were dried over anhydrous Na$_2$SO$_4$ and concentrated in vacuo. The crude residue was chromatographed with CHCl$_3$/MeOH (95:5) as eluent, to give **4b** as a pale-yellow semisolid (0.04 g, 48% yield). ^{1}H NMR (CDCl$_3$): δ 0.88 (t, 3H, J=7.3 Hz), 1.41–1.50 and 1.71–1.83 (m, 12H), 1.92–1.97 (m, 1H), 2.34–2.42 (m, 6H), 2.77–2.99 (m, 6H), 3.29 (br s, 1H, D$_2$O exchanged), 3.81 (s, 3H), 6.19 (br d, 1H), 6.65–6.72 (m, 2H), 7.11 (t, 1H, J=7.8 Hz), 8.47 (d, 1H, J=8.2 Hz). HRMS (ESI$^+$) calcd for [(C$_{26}$H$_{35}$N$_5$O$_4$+H]$^+$: 482.2762, found: 482.2773.

5-(Dimethylamino)-N-[5-[(8-hydroxy-1,2,3,4-tetrahydronaphtalen-2-yl)(propyl)amino]pentyl]naphtalen-1-sulfonamide (5a). To a stirred solution of **4a** (0.15 g, 0.27 mmol) in anhydrous CH$_2$Cl$_2$ (10 mL) cooled at 0°C, a 1 M solution of boron tribromide in CH$_2$Cl$_2$ (0.47 mL) was added. The reaction mixture was stirred at room temperature for 4 h, then was poured into ice cooled conc. NH$_4$OH solution (20 mL). The separated organic layer was washed with brine (20 mL), dried over anhydrous Na$_2$SO$_4$, and concentrated in vacuo. The crude residue was purified through flash chromatography (gradient elution from 5% to 10% MeOH in CHCl$_3$), to give **5a** as a brown solid (0.12 g, 69% yield). ^{1}H-NMR (CD$_3$OD): δ 0.87 (t, 3H, J=7.3 Hz), 1.32–1.41 and 1.51–1.76 (m, 12H), 1.90–1.95 (m, 1H), 2.34–2.42 (m, 6H), 2.77–2.99 (m+s, 10H), 6.67 (dd, 2H, J=7.8 Hz), 7.07 (t, 1H, J=7.8 Hz), 7.17 (d, 1H, J=7.3 Hz), 7.50–7.56 (m, 2H), 8.23–8.29 (m, 2H), 8.52 (d, 1H, J=8.8 Hz). HRMS (ESI$^-$) calcd for [(C$_{32}$H$_{45}$N$_3$O$_3$S–H]$^-$: 536.2952, found: 536.2942.

N-[5-[(8-Hydroxy-1,2,3,4-tetrahydronaphnthalen-2-yl)(propyl)amino]pentyl]-7-nitrobenzene[c][1,2,5]oxadiazol-4-sulfonamide (5b). The title compound was obtained starting from **4b** (0.13 g, 0.27 mmol), following the same procedure described for the synthesis of **5a**, as a brown semisolid in 60% yield. ^{1}H-NMR (CD$_3$OD): δ 0.89 (t, 3H, J=7.3 Hz), 1.41–1.50 and 1.71–1.83 (m, 12H), 1.92–1.97 (m, 1H), 2.34–2.42 (m, 6H), 2.77–2.99 (m, 6H), 6.19 (br d, 1H), 6.65–6.72 (m, 2H), 7.11 (t, 1H, J=7.8 Hz), 8.47 (d, 1H, J=8.2 Hz). HRMS (ESI$^-$) calcd for [(C$_{25}$H$_{33}$N$_5$O$_4$–H]$^-$: 466.2460, found: 466.2446.

Radioligand binding assay at human cloned 5-HT$_{1A}$R

HEK293 cell line with stable expression of human 5-HT$_{1A}$R (prepared with the use of Lipofectamine 2000) was maintained at 37°C in a humidified atmosphere with 5% CO$_2$ and grown in Dulbecco's Modified Eagle Medium containing 10% dialyzed fetal bovine serum and 500 μg/mL G418 sulfate. For membrane preparation, cells were sub-cultured in 150 cm^2 flasks, grown to 90% confluence, washed twice with prewarmed to 37°C phosphate-buffered saline (PBS), and pelleted by centrifugation (200 g) in PBS containing 0.1 mM ethylenediaminetetraacetic acid (EDTA) and 1 mM dithiothreitol (DTT). Before membrane preparation, pellets were stored at −80°C.

The cell pellet was thawed and homogenized in 10 volumes of assay buffer using an Ultra Turrax tissue homogenizer and centrifuged twice at 35000 g for 15 min at 4°C, with incubation for 15 min at 37°C in between. According to the previously published procedure,[40] the experiments were carried out using 2.5 nM [^{3}H]8-OH-DPAT (135.2 Ci/mmol, PerkinElmer, USA). The composition of the assay buffer includes 50 mM Tris HCl, 0.1 mM EDTA, 4 mM MgCl$_2$, 10 μM pargyline and 0.1% ascorbate. The assay was incubated in a total volume of 200 μL in 96-well microtiter plates for 1 h at room temperature with gentle shaking. The process of equilibration was terminated by rapid filtration through Unifilter plates with a Unifilter-96 Cell Harvester (PerkinElmer, USA) and radioactivity retained on the filters was quantified on a Microbeta plate reader (PerkinElmer, USA). Non-specific binding was defined with 10 μM of 5-HT. Each compound was tested in triplicate at 7 concentrations (10^{-10}–10^{-4} M). The final assay concentration of DMSO was 1%. The inhibition constants (K_i) were calculated from the Cheng-Prusoff equation[41] using GraphPad Prism 9 program. Results were expressed as means of two separate experiments.

Fluorescence spectroscopy

To determine the maximum absorption wavelength, the UV/Vis absorption spectra of compounds **5a,b** were recorded in the wavelength range between 190 nm and 700 nm using a Shimadzu UV-1800 spectrophotometer. The emission spectra were recorded in the wavelength range between 300 and 800 nm, progressively exciting at values of λ included in the ±20 nm range with respect to the λmax of absorption, as detailed in Figures S5 and S6. The excitation spectra were recorded using the Tecan Infinite M1000 Pro Microplate reader.

Cell Culture

Human islets, isolated from cadaveric nondiabetic donors, were obtained from the Integrated Islet Distribution Program (IIDP) (City of Hope National Medical Center, Duarte, CA, USA). The average purity and viability of the islets obtained from control donors (n= 6) was 90±2%. Upon receipt, the isolated human islets were cultured in supplemented CMRL-1066 media for no longer than 1 day, followed by washing and then dissociated in 0.05% trypsin/EDTA solution. The dissociated islets were filtered through a sterile 40 μm nylon filter and collected and washed in minimum essential medium (M.E.M.) with GlutaMAX (Gibco), 12 mM glucose, 5% F.B.S., 1 mM sodium, pyruvate, 10 mM HEPES, 100 U/mL penicillin and 100 U/mL streptomycin and 1× B-27 Supplement (Gibco, Gaithersburg, MD, USA). Cells were seeded at 10,000–20,000 cells/cm2 on Collagen IV (Millipore Sigma) coated coverslip chambers (Cellvis, Mountain View, CA, USA) in the same medium and allowed to reach full adherence (4–5 days) before live cell imaging or immunohistochemistry. Cells were incubated in "imaging media" consisting of phenol red free RPMI 1640. media (Caisson Labs, Smithfield, UT, USA) supplemented with 95 mg/100 mL defatted bovine serum albumin (BSA), 1 mL/100 mL Pen-Strep 100× solution (Corning), 84 mg/100 mL sodium bicarbonate, 5 mM HEPES, and 12 mM glucose) supplemented with the indicated fluorescent probe. Cultures were incubated in the dark for 40–45 minutes at room temperature, washed twice with imaging media without probes, and then incubated with FluoroBrite™ DMEM (Thermo Fisher Scientific, Fair Lawn, NJ, USA) at 37°C in a humidified 5% CO$_2$ atmosphere during imaging.

Immunochemistry

Immunocytochemistry was performed on human pancreatic islet cells grown as previously described.[32,36] Monolayer cultures were washed in phosphate buffered saline (PBS) and fixed with 4% EM-grade paraformaldehyde in PBS (Electron Microscopy Sciences) at room temperature for 15 minutes. Samples were permeabilized in PBS+0.3% Triton X-100 and blocked with PBS+0.2% Triton X-100

ChemMedChem

Research Article

doi.org/10.1002/cmdc.202100759

**Chemistry
Europe**

European Chemical
Societies Publishing

with 10% goat or rabbit serum for 60 minutes at room temperature. Primary antibodies were incubated overnight at 4 °C. Alexa Fluor conjugated secondary antibodies (Invitrogen) were incubated in 0.3% Triton X-100 in PBS plus B.S.A. for 60 minutes at room temperature. Coverslips were mounted with Vectashield HardSet Antifade Mounting Medium with DAPI (Vector labs, Burlingame, CA, USA). The following primary antibodies and dilutions were used for immunofluorescent staining: Anti-Human Insulin 1:100 (Invitrogen/53976980) conjugated to AF 488, Mouse monoclonal Ab, Anti-Insulin mouse monoclonal antibody, 1:1000 (Boster/#M00067-1) (for rat pancreas) Anti-Glucagon 1:100 (Boster/MA1047) Mouse monoclonal Ab. Anti-Human; Rat 5-HT1A Receptor/HTR1A Rabbit IgG polyclonal Antibody 1:1000 (Boster/#PA1647) Anti-Human; Rat 5-HT2A Receptor/HTR2A Rabbit IgG polyclonal antibody, 1:1000 (Boster/#PB9599). The secondary antibodies used in these experiments were Anti Rabbit IgG 1:2000 (Sigma Aldrich/SAB4600426) conjugated to CF 568 and Anti-Rabbit IgG 1:2000 (Sigma Aldrich/F9384) conjugated to FITC. Immunohistochemistry on formaldehyde-fixed paraffin-embedded sections was performed with the same antibodies and sections were prepared using standard methods.

Microscopy

A Zeiss Axiovert 135 inverted epifluorescence microscope fitted with two independently controlled collimated light sources, 5.1 W Solis 385 nm L.E.D. or a 4.2 W Solis 400–700 nm L.E.D.s (Thorlabs Inc., Newton, NJ) and Zeiss a 50× L.D. EC Epi-plan-Neofluar (0.55 NA), 63× A Plan (0.8) and 100× Plan Neofluar (1.3 NA) objectives were used to obtain cell images. Specific excitation and emission wavelengths were obtained with the following filter sets; A) Excitation 330WB80, Dichroic 400DCLP, Emission 450BP80 (used for DAPI and the fluoroprobe **5a**), B) Excitation 470QM40, Dichroic 505 DRLP, Emission 535QM50 (used for FluoZin-3 AM or NeuroSensor 521) C) Excitation 560QM55, Dichroic 595 DCLP, Emission 645QM75 (used for LysoTracker Red DND-99 and Nuclear Mask Deep Red) (all from Omega Optical, Brattleboro, VT, USA). The fluoroprobe **5a** was first imaged using the 385 nm source. Then, the 385 nm source was extinguished and the broadband 400–700 nm source was turned on for subsequent image acquisition. In this optical system, at 100× magnification under oil, the x–y resolution was around 220 nm (given by the Abbe limit) and the depth of field of approximately 250 nm (given by the Shillaber equation). Under these culture conditions, most cells could be captured in their entirety using a single focal plane. Images were projected onto a Lumenera Infinity 2 monochrome 2 megapixel camera (Ottawa, Ontario, Canada) and acquired with Lumenera Infinity Capture or IMAGEJ software. Image data were exported as single 1392×1040 pixels, 16-bit greyscale TIFF files and further processed using IMAGEJ[38] and/or OpenCFU.[42] The size of objects within the images captured was obtained via calibration by ImageJ software with a stage micrometer (0.1 mm in 0.002 mm divisions) (Ted Pella, Inc., Redding, CA, USA). WAY-100635 was from Sigma Aldrich (Sigma Aldrich Inc., USA).

Conflict of Interest
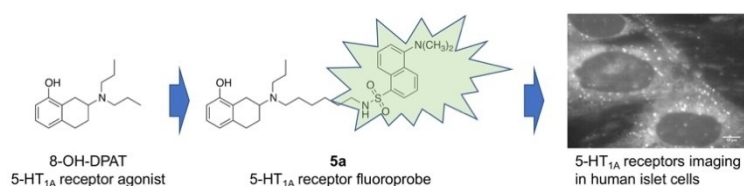
The authors declare no conflict of interest.

Data Availability Statement

The data that support the findings of this study are available from the corresponding author upon reasonable request.

[1] D. D. Lam, L. K. Heisler, *Expert Rev. Mol. Med.* **2007**, *9*, 1–24.
[2] F. Sundler, R. Hakanson, I. Loren, I. Lundquist, *Invest. Cell Pathol.* **1980**, *3*, 87–103.
[3] L. Cegrell, *Acta Physiol. Scand. Suppl.* **1968**, *314*, 1–60.
[4] O. Kwon, J. H. Yu, E. Jeong, H. J. Yoo, M. S. Kim, *Clin. Endocrinol.* **2018**, *88*, 549–555.
[5] L. R. Cataldo Bascuñan, C. Lyons, H. Bennet, I. Artner, M. Fex, *Acta Physiol.* **2019**, *225*, e13101.
[6] N. M. Barnes, G. P. Ahern, C. Becamel, J. Bockaert, M. Camilleri, S. Chaumont-Dubel, S. Claeysen, K. A. Cunningham, K. C. Fone, M. Gershon, G. Di Giovanni, N. M. Goodfellow, A. L. Halberstadt, R. M. Hartley, G. Hassaine, K. Herrick-Davis, R. Hovius, E. Lacivita, E. K. Lambe, M. Leopoldo, F. O. Levy, S. C. R. Lummis, P. Marin, L. Maroteaux, A. C. McCreary, D. L. Nelson, J. F. Neumaier, A. Newman-Tancredi, H. Nury, A. Roberts, B. L. Roth, A. Roumier, G. J. Sanger, M. Teitler, T. Sharp, C. M. Villalón, H. Vogel, S. W. Watts, D. Hoyer, *Pharmacol. Rev.* **2021**, *73*, 310–520.
[7] H. Bennet, I. G. Mollet, A. Balhuizen, A. Medina, C. Nagorny, A. Bagge, J. Fadista, E. Ottosson-Laakso, P. Vikman, M. Dekker-Nitert, L. Eliasson, N. Wierup, I. Artner, M. Fex, *Diabetologia* **2016**, *59*, 744–754.
[8] L. R. Cataldo, V. A. Cortés, J. E. Galgani, P. R. Olmos, J. L. Santos, *Nutr. Hosp.* **2014**, *30*, 498–508. ■■Dear author, please check the journal-title!!■■
[9] N. Paulmann, M. Grohmann, J. P. Voigt, B. Bert, J. Vowinckel, M. Bader, M. Skelin, M. Jevsek, H. Fink, M. Rupnik, D. J. Walther, *PLoS Biol.* **2009**, *7*, e1000229.
[10] H. Chen, F. Hong, Y. Chen, J. Li, Y. S. Yao, Y. Zhang, L. F. Zheng, J. X. Zhu, *Eur. J. Pharmacol.* **2016**, *789*, 354–361.
[11] B. Coulie, J. Tack, R. Bouillon, T. Peeter, J. Janssens, *Am. J. Physiol.* **1998**, *274*, E317–20.
[12] Q. Zhang, Y. Zhu, W. Zhou, L. Gao, L. Yuan, X. Han, *PLoS One* **2013**, e54250.
[13] J. Marco, J. A. Hedo, M. L. Villanueva, *Diabetologia* **1977**, *13*, 585–588.
[14] J. Almaça, J. Molina, D. Menegaz, A. N. Pronin, A. Tamayo, V. Slepak, P. O. Berggren, A. Caicedo, *Cell Rep.* **2016**, *17*, 3281–3291.
[15] M. Ohara-Imaizumi, H. Kim, M. Yoshida, T. Fujiwara, K. Aoyagi, Y. Toyofuku, Y. Nakamichi, C. Nishiwaki, T. Okamura, Y. Fujitani, K. Akagawa, M. Kakei, H. Watada, M. S. German, S. Nagamatsu, *Proc. Natl. Acad. Sci. USA* **2013**, *110*, 19420–19425.
[16] D. Švob Štrac, N. Pivac, D. Mück-Šeler, *Transl. Neurosci.* **2016**, *7*, 35–49. ■■Dear author, please check the journal-title!!■■
[17] M. D. Guenette, A. Giacca, M. Hahn, C. Teo, L. Lam, A. Chintoh, T. Arenovich, G. Remington, *Schizophr. Res.* **2013**, *146*, 162–169. ■■Dear author, please check the journal-title!!■■
[18] M. Hahn, A. Chintoh, A. Giacca, L. Xu, L. Lam, S. Mann, P. Fletcher, M. Guenette, T. Cohn, T. Wolever, T. Arenovich, G. Remington, *Schizophr. Res.* **2011**, *131*, 90–95. ■■Dear author, please check the journal-title!!■■
[19] R. Isaac, S. Boura-Halfon, D. Gurevitch, A. Shainskaya, Y. Levkovitz, Y. Zick, *J. Biol. Chem.* **2013**, *288*, 5682–93.

[20] M. Leopoldo, E. Lacivita, F. Berardi, R. Perrone, *Drug Discovery Today* **2009**, *14*, 706–712.

[21] E. Lacivita, M. Leopoldo M, *J. Med. Chem.* **2008**, *51*, 1492–1495.

[22] E. Lacivita, M. Leopoldo, A. C. Masotti, C. Inglese, F. Berardi, R. Perrone, S. Ganguly, M. Jafurulla, A. Chattopadhyay, *J. Med. Chem.* **2009**, *52*, 7892–7896.

[23] E. Lacivita, A. C. Masotti, M. Jafurulla, R. Saxena, N. Rangaraj, A. Chattopadhyay, N. A. Colabufo, F. Berardi, R. Perrone, M. Leopoldo, *Bioorg. Med. Chem. Lett.* **2010**, *20*, 6628–6632.

[24] D. Alonso, H. Vázquez-Villa, A. M. Gamo, M. F. Martínez-Esperón M F Tortosa, A. Viso, R. Fernández de la Pradilla, E. Junquera, E. Aicart, M. Martín-Fontecha, B. Benhamú, M. L. López-Rodríguez, S. Ortega-Gutiérrez, *ACS Med. Chem. Lett.* **2010**, *1*, 249–253.

[25] L. Töntson, S. Kopanchuk, A. Rinken, *Neurochem. Int.* **2014**, 67, 32–38.

[26] G. Hernández-Torres, E. Enríquez-Palacios, M. Mecha, A. Feliú, A. Rueda-Zubiaurre, A. Angelina, L. Martín-Cruz, M. Martín-Fontecha, O. Palomares, C. Guaza, E. Peña-Cabrera, M. L. López-Rodríguez, S. Ortega-Gutiérrez, *Bioconjugate Chem.* **2018**, *29*, 2021–2027.

[27] T. J. Pucadyil, S. Kalipatnapu, A. Chattopadhyay, *Cell. Mol. Neurobiol.* **2005**, *25*, 553–580.

[28] E. Lacivita, M. Leopoldo, F. Berardi, R. Perrone, *Curr. Top. Med. Chem.* **2008**, *8*, 1024–1034.

[29] V. Bakthavachalam, J. B. Fell, M. Teitler, R. A. Glennon, J. L. Neumeyer, *Med. Chem. Res.* **1991**, *1*, 265–270.

[30] N. Naiman, R. A. Lyon, A. E. Bullock, L. T. Rydelek, M. Titeler, R. A. Glennon, *J. Med. Chem.* **1989**, *32*, 253–256.

[31] M. J. Millan, A. Newman-Tancredi, V. Audinot, D. Cussac, F. Lejeune, J. P. Nicolas, F. Cogé, J. P. Galizzi, J. A. Boutin, J. M. Rivet, A. Dekeyne, A. Gobert, *Synapse* **2000**, 35, 79–95.

[32] E. A. Phelps, C. Cianciaruso, J. Santo-Domingo, M. Pasquier, G. Galliverti, L. Piemonti, E. Berishvili, O. Burri, A. Wiederkehr, J. A. Hubbell, S. Baekkeskov, *Sci. Rep.* **2017**, *7*, 45961.

[33] E. A. Forster, I. A. Cliffe, D. J. Bill, G. M. Dover, D. Jones, Y. Reilly, A. Fletcher, *Eur. J. Pharmacol.* **1995**, *281*, 81–88.

[34] X. Khawaja, N. Evans, Y. Reilly, C. Ennis, M. C. Minchin, *J. Neurochem.* **1995**, *64*, 2716–2726.

[35] L. S. Tompkins, K. D. Nullmeyer, S. M. Murphy, C. S. Weber, R. M. Lynch, *Am. J. Physiol. Cell Physiol.* **2002**, *283*, C429–437.

[36] S. Pecic, N. Milosavic, G. Rayat, A. Maffei, P. E. Harris, *Sci. Rep.* **2019**, *9*, 5403.

[37] V. Palivec, C. M. Viola, M. Kozak, T. R. Ganderton, K. Křížková, J. P. Turkenburg, P. Halušková, L. Žáková, J. Jiráček, P. Jungwirth, A. M. Brzozowski, *J. Biol. Chem.* **2017**, *292*, 8342–8355.

[38] C. A. Schneider, W. S. Rasband, K. W. Eliceiri, *Nat. Methods* **2012**, 9, 671–675.

[39] S. Asad, P. Nikamo, A. Gyllenberg, H. Bennet, O. Hansson, N. Wierup, Diabetes Incidence in Sweden Study Group, A. Carlsson, G. Forsander, S. A. Ivarsson, H. Larsson, Å Lernmark, B. Lindblad, J. Ludvigsson, C. Marcus, K. S. Rønningen, J. Nerup, F. Pociot, H. Luthman, M. Fex, I. Kockum, *PLoS One.* **2012**, *7*, e35439.

[40] P. Zajdel, T. Kos, K. Marciniec, G. Satała, V. Canale, K. Kamiński, M. Hołuj, T. Lenda, R. Koralewski, M. Bednarski, L. Nowiński, J. Wójcikowski, W. A. Daniel, A. Nikiforuk, I. Nalepa, P. Chmielarz, J. Kuśmierczyk, A. J. Bojarski, P. Popik, *Eur. J. Med. Chem.* **2018**, *145*, 790–804.

[41] Y. Cheng, W. H. Prusoff, *Biochem. Pharmacol.* **1973**, *22*, 3099–3108.

[42] Q. Geissmann, *PLoS One* **2013**, *8*, e54072.

RESEARCHARTICLE

8-OH-DPAT
5-HT$_{1A}$ receptor agonist

5a
5-HT$_{1A}$ receptor fluoroprobe

5-HT$_{1A}$ receptors imaging
in human islet cells

R. W. Garvey, Prof. E. Lacivita*,
Dr. M. Niso, Dr. B. Duszyńska,
Prof. P. E. Harris, Prof. M. Leopoldo

1 – 11

Design, Synthesis, and Characterization of a Fluoroprobe for Live Human Islet Cell Imaging of Serotonin 5-HT$_{1A}$ Receptor

We have developed a high-affinity green-emitting fluorescent probe for the serotonin 5-HT$_{1A}$ receptor used for first-time imaging of the 5-HT$_{1A}$ receptor in live human islet cells. 5-HT$_{1A}$ receptors are colocalized with insulin in human β-cells and with glucagon in human α-cell vesicles.

 ## SPACE RESERVED FOR IMAGE AND LINK

Share your work on social media! *ChemMedChem* has added Twitter as a means to promote your article. Twitter is an online microblogging service that enables its users to send and read short messages and media, known as tweets. Please check the pre-written tweet in the galley proofs for accuracy. If you, your team, or institution have a Twitter account, please include its handle @username. Please use hashtags only for the most important keywords, such as #catalysis, #nanoparticles, or #proteindesign. The ToC picture and a link to your article will be added automatically, so the **tweet text must not exceed 250 characters**. This tweet will be posted on the journal's Twitter account (follow us @ChemMedChem) upon publication of your article in its final (possibly unpaginated) form. We recommend you to re-tweet it to alert more researchers about your publication, or to point it out to your institution's social media team.

ORCID (Open Researcher and Contributor ID)

Please check that the ORCID identifiers listed below are correct. We encourage all authors to provide an ORCID identifier for each coauthor. ORCID is a registry that provides researchers with a unique digital identifier. Some funding agencies recommend or even require the inclusion of ORCID IDs in all published articles, and authors should consult their funding agency guidelines for details. Registration is easy and free; for further information, see http://orcid.org/.

Robert W. Garvey
Prof. Enza Lacivita http://orcid.org/0000-0003-2443-1174
Dr. Mauro Niso
Dr. Beata Duszyńska
Prof. Paul E. Harris
Prof. Marcello Leopoldo